

# Infall, Fragmentation and Outflow in Sgr B2

**Sheng-Li Qin<sup>1,2</sup>, Jun-Hui Zhao<sup>1</sup>, James M. Moran<sup>1</sup>, Daniel Marrone<sup>1</sup>,  
N. Patel<sup>1</sup>, Sheng-Yuan Liu<sup>3</sup>, Yi-Jehng Kuan<sup>3,4</sup>, Jun-Jie Wang<sup>2</sup>**

<sup>1</sup> Harvard-Smithsonian Center for Astrophysics, 60 Garden St, Cambridge, MA 02138, USA

<sup>2</sup> National Astronomical Observatories, CAS, Beijing, 100012, P. R. China

<sup>3</sup> Academia Sinica Institute of Astronomy and Astrophysics, Taipei 106, Taiwan

<sup>4</sup> Department of Earth Sciences, National Taiwan Normal University, Taipei 116, Taiwan

E-mail: `sqin@cfa.harvard.edu`

**Abstract.** Observations of H<sub>2</sub>CO lines and continuum at 1.3 mm towards Sgr B2(N) and Sgr B2(M) cores were carried out with the SMA. We imaged H<sub>2</sub>CO line absorption against the continuum cores and the surrounding line emission clumps. The results show that the majority of the dense gas is falling into the major cores where massive stars have been formed. The filaments and clumps of the continuum and gas are detected outside of Sgr B2(N) and Sgr B2(M) cores. Both the spectra and moment analysis show the presence of outflows from Sgr B2(M) cores. The H<sub>2</sub>CO gas in the red-shifted outflow of Sgr B2(M) appears to be excited by a non-LTE process which might be related to the shocks in the outflow.

## 1. Introduction

The giant molecular cloud Sgr B2 is located in the Galactic center ( $\sim 44'$  from SgrA\*). High resolution radio continuum and recombination line observations at centimeter wavelenghts showed the two most active star forming cores, Sgr B2(N) and (M), hosting clusters of massive stars associated with UCHII regions [1-6]. Previous observations showed that massive star formation is taking place in both Sgr B2(N) and (M), suggesting that the two hot cores are at different evolutionary stages [7-12]. H<sub>2</sub>CO molecule has a simple chemical formation path and has been proven to be a useful probe of physical conditions of star formation regions [13,14]. We observed Sgr B2 at 1.3 mm with the SMA including the lines of H<sub>2</sub>CO. The new results regarding the ongoing star formation in the Galactic center region are reported in this paper.

## 2. Observations and Results

Two fields centered on Sgr B2(N) and (M) were observed at 1.3 mm with the SMA<sup>1</sup> in the compact configuration on August 1, 2005. Three H<sub>2</sub>CO transitions were included in the 2 GHz sideband, one of them is blended with other molecular lines. The two unblended transitions are the H<sub>2</sub>CO ( $3_{03} - 2_{02}$ ) and ( $3_{21} - 2_{20}$ ) with upper level energies ( $E_u$ ) of 21.0 K and 67.8 K at the rest frequencies 218.222 and 218.760 GHz, respectively. The data reduction including calibration, imaging and analysis was carried out using *Miriad*. The continuum subtraction was

<sup>1</sup> The Submillimeter Array is a joint project between the Smithsonian Astrophysical Observatory and the Academia Sinica Institute of Astronomy and Astrophysics and is funded by the Smithsonian Institution and the Academia Sinica.

made in the UV domain using UVLIN. The mosaic of Sgr B2(N) and Sgr B2(M) was made using a simple linear mosaicing algorithm. The primary beam attenuation was also corrected.

The mosaic of the continuum images of Sgr B2 with an angular resolution of  $5.^{\circ}4 \times 3.^{\circ}2$  is shown in Fig. 1, showing the two bright components Sgr B2(N) ( $S_p=29.2 \pm 0.1$  Jy beam $^{-1}$ ) and Sgr B2(M) ( $S_p=20.2 \pm 0.1$  Jy beam $^{-1}$ ). The continuum sources associated with the UCHII regions K1, K2 and K3 in the Sgr B2(N) core are not resolved at this angular resolution. However a few continuum clumps have been detected, namely, Sgr B2(N)-E ( $S_p=1.1 \pm 0.1$  Jy beam $^{-1}$ ), Sgr B2(N)-W ( $S_p=1.0 \pm 0.1$  Jy beam $^{-1}$ ) and K4 ( $S_p=1.4 \pm 0.1$  Jy beam $^{-1}$ ). We have checked previous observations at longer wavelengths and have found no radio continuum sources to be associated with Sgr B2(N)-E and Sgr B2(N)-W, indicating that the continuum emission at 1.3 mm arises mainly from dust and the two clumps are probably in an early stage of star formation. The strong continuum emission from the unresolved Sgr B2(M) core mainly arises from the UCHII regions F1, F2, F3 and F4. In addition, a continuum component (Sgr B2(M)-W,  $S_p=1.7 \pm 0.1$  Jy beam $^{-1}$ ) is located west of the Sgr B2(M) core. The position of the continuum peak at 1.3 mm of the Sgr B2(M)-W is consistent with that of the source B at 3.8 mm [9] and contains components A1 and A2 at 1.3 cm [2]. Finally, a component, associated with the UCHII region Z10.24, is detected at 1.3 mm ( $S_p=2.0 \pm 0.1$  Jy beam $^{-1}$ ), revealing a filamentary morphology located between Sgr B2(N) and (M).

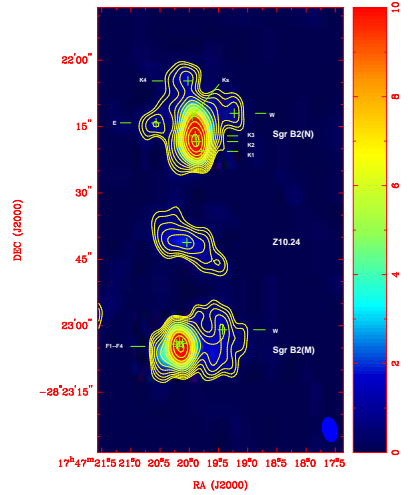


**Figure 1.** The mosaic of the Sgr B2 continuum image at 1.3 mm by combining 218 (LSB) and 228 GHz (USB) data. The synthesized beam is  $5.^{\circ}4 \times 3.^{\circ}2$ , PA=12.5° (lower-right corner). The wedge indicates the intensity scale from 0 to 10 Jy beam $^{-1}$ . The contours are -4, 4, 5.66, 8, 11.3, 16, 22.63, 32, 45.25, 64, 90.51, 128, 181.26  $\sigma$ . The rms (1  $\sigma$ ) is 0.1 Jy beam $^{-1}$ .

The integrated H<sub>2</sub>CO line emission flux images are shown in Fig. 2. Most of the emission is distributed around the two cores with peak line emission flux of  $F_{3_{03}-2_{02}}=653$  Jy beam $^{-1}$  km s $^{-1}$  and  $F_{3_{21}-2_{20}}=696$  Jy beam $^{-1}$  km s $^{-1}$  for Sgr B2(N), and  $F_{3_{03}-2_{02}}=92.6$  Jy beam $^{-1}$  km s $^{-1}$  and  $F_{3_{21}-2_{20}}=94.7$  Jy beam $^{-1}$  km s $^{-1}$  for Sgr B2(M). Clearly, the distribution of the H<sub>2</sub>CO gas is not spherically symmetric with respect to each of the two star formation cores. In Sgr B2(N) region, in addition to the gas concentration on the core, there are a few clumps of gas distributed in the vicinity. We note that the emission images of the two transitions have a very similar morphology in the Sgr B2(N) region. In Sgr B2(M), the brightest emission of the higher transition gas is located 5'' SE of the continuum peak while the peak emission of the lower transition gas coincides with the continuum peak, suggesting that the two transitions in Sgr B2(M) correspond to different physical conditions. Most of the gas traced by low transition H<sub>2</sub>CO line in Sgr B2(M) is located NW of the core, showing filamentary and clumpy structures.

The typical spectra at several positions are made from channel maps. The spectra towards the two continuum peaks in Sgr B2(N) and (M), show the gas components in either absorption

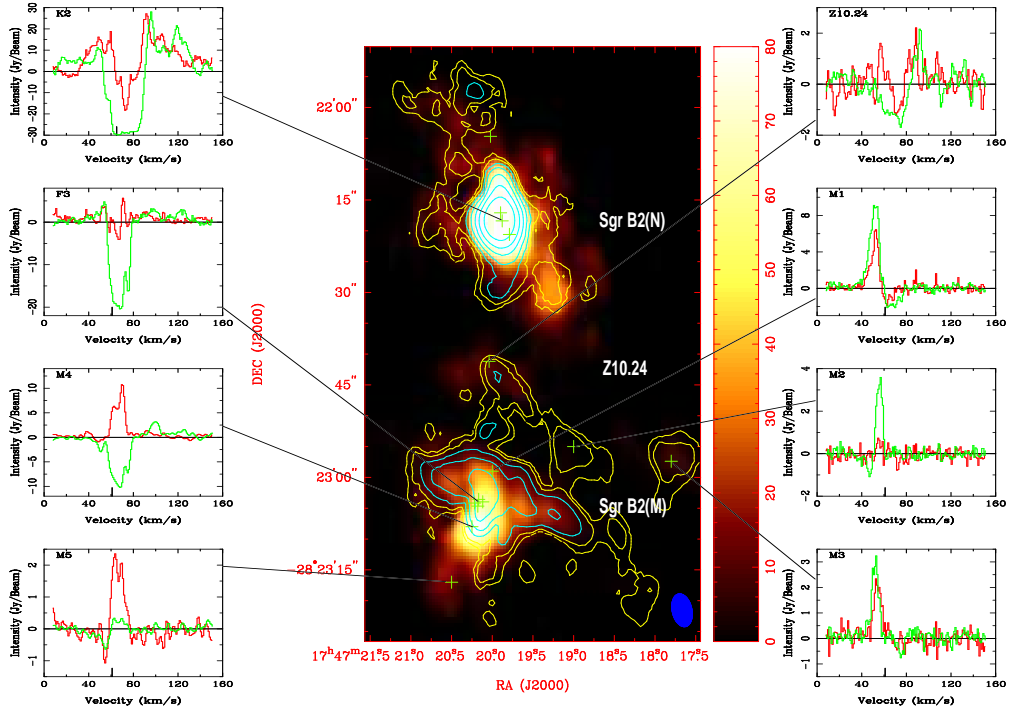


**Figure 2.** Middle panel is the mosaic images of the integrated intensities of  $\text{H}_2\text{CO}$  ( $3_{21} - 2_{20}$ ) (pseudo-color in a scale range from 0 to 80  $\text{Jy beam}^{-1} \text{ km s}^{-1}$ ) and  $\text{H}_2\text{CO}$  ( $3_{03} - 2_{02}$ ) (contours 4,8,16,32,64,128,256  $\text{Jy beam}^{-1} \text{ km s}^{-1}$ ) with FWHM beam of  $5.^{\prime\prime}4 \times 3.^{\prime\prime}2$ , PA= $12^{\circ}.5$ . The left and right panels are the spectra at the positions of the various components for the low transition  $3_{03} - 2_{02}$  (green) and the high transition  $3_{21} - 2_{20}$  (red), respectively. The horizontal line is the zero level after continuum-subtraction, and the vertical thick bars mark the systematic velocity of the sources. The systematic velocities are 65 and 61  $\text{km s}^{-1}$  for Sgr B2(N) and Sgr B2(M), respectively.

or emission. The absorbing gas associated with two cores is dominated by the red-shifted gas with respect to the systematic velocity, suggesting that the gas is moving towards the cores. The spectrum of the higher transition emission at K2 shows three absorbing peaks at velocity 66.0, 73.0 and 80.4  $\text{km s}^{-1}$ , respectively, while the absorbing intensities of the lower transition appear to be saturated. The observed line intensity ( $F_{\nu}$ ), the linewidth ( $\Delta V$ ), the ratios of L/C and the ratio of  $F_{303-202}/F_{321-220}$  give a strong constraint on the physical condition. Considering the excitation condition and opacity effect of the two transitions, the kinetic temperature of 40-50 K and  $\text{H}_2$  density of  $10^7 \text{ cm}^{-3}$  are suggested by a large-velocity-gradient (LVG) model for the absorbing gas in the core. The lower transition spectrum at F3 shows two absorbing peaks near 65 and 75  $\text{km s}^{-1}$  while the high transition spectrum show the absorption near 65  $\text{km s}^{-1}$  and emission peak near 75  $\text{km s}^{-1}$ . The multiple velocity components of the spectra in both absorption and emission appear to indicate that there are multiple gas clumps located at different depths inside the two cloud cores. High spatial resolution  $\text{H}_2\text{CO}$  line observations will be a critical key to resolve the gas kinematics of the multiple components in the two cores.

The lower transition  $\text{H}_2\text{CO}$  ( $3_{03} - 2_{02}$ ) spectrum of Z10.24 shows that most of the gas is in absorption with a broad line width ( $\sim 50 \text{ km s}^{-1}$ ) and the emission is red-shifted with respect to the absorption, while the spectrum of the higher  $\text{H}_2\text{CO}$  transition shows a doubly peaked profile

with an absorbing dip at  $65 \text{ km s}^{-1}$  which is consistent with optically thin radio recombination line H66 $\alpha$  observations [5]. De Pree et al. (1996) [5] argued that an ionized outflow is centered on Z10.24. The P-cygni profile in H<sub>2</sub>CO (3<sub>03</sub> – 2<sub>02</sub>) spectrum and doubly peaked profile in H<sub>2</sub>CO (3<sub>21</sub> – 2<sub>20</sub>) spectrum appear to favor the argument of an outflow from the UCHII region. The M1 located within the continuum core shows an inverse P-cygni profile in the spectra of both H<sub>2</sub>CO transitions, providing evidence for the gas moving into the core. M2 located within the filament (30" in length and 7" in width) shows significant emission ( $30 \sigma$  in the peak line intensity) in the lower transition while the higher transition line emission is less significant (2-3  $\sigma$ ), suggesting that the gas is cold in this extended arclike structure. The line emission of both transitions from clumps M3 is detected ( $> 15 \sigma$ ).

M4 and M5 reside in the outflow region of Sgr B2(M) [8, 11]. At M4 near the core, the spectra show that the high transition gas is in emission while the low transition gas is in absorption against the continuum. Most of the lower transition gas in absorption, which appears to be red-shifted with respect to the systematic velocity, is evident for the gas infalling into the core while the higher transition gas in red-shifted emission is suggested to be the outflow gas from the core. M5 is located at the tip of the outflow, where the spectrum shows a very significant line emission ( $20 \sigma$ ) of the higher transition gas with a linewidth of  $\sim 20 \text{ km s}^{-1}$ , composed of at least two velocity components while less significant emission (2-3  $\sigma$ ) of the lower transition gas is shown at the same spot, suggesting that the molecular gas does not satisfy the LTE condition. The H<sub>2</sub>CO gas in the outflow appears to be excited by a non-LTE process, which might be related to the shocks in the outflow. The shocks could be C-shock if the gas is weakly ionized and shock velocity is below critical value  $\sim 50 \text{ km s}^{-1}$  [15]. M5 is far away from the continuum at cm wavelengths and the H<sub>2</sub>CO line width is below  $20 \text{ km s}^{-1}$ . The high transition H<sub>2</sub>CO (3<sub>21</sub>-2<sub>20</sub>) in Sgr B2(M) outflow appears to be excited by a C-shock.

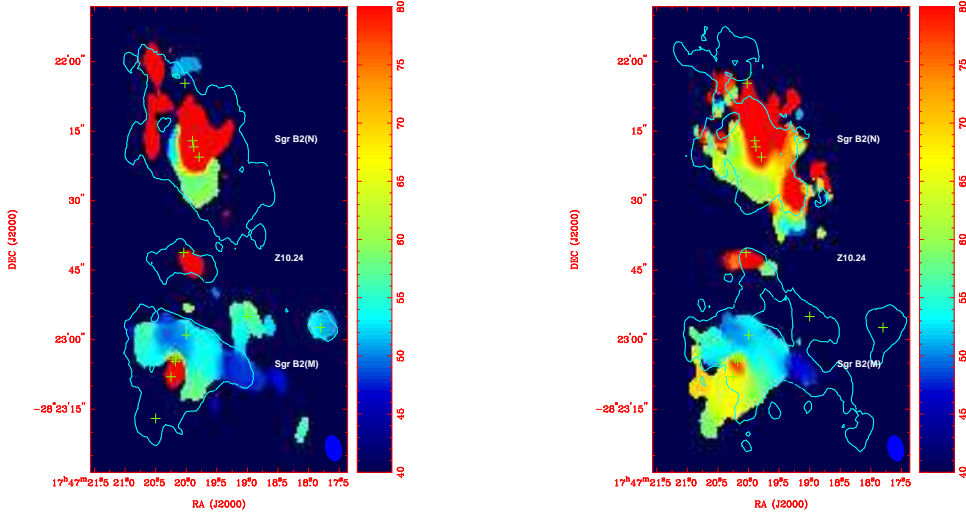


**Figure 3.** The mosaic images of the intensity weighted velocity constructed using a cutoff of  $8 \sigma$  for the H<sub>2</sub>CO (3<sub>03</sub> – 2<sub>02</sub>) emission (color) overlaid with the contours of H<sub>2</sub>CO (3<sub>21</sub> – 2<sub>20</sub>) intensity on the left panel. The right panel is the velocity field of the H<sub>2</sub>CO (3<sub>21</sub> – 2<sub>20</sub>) emission (color) overlaid with the contours of H<sub>2</sub>CO (3<sub>03</sub> – 2<sub>02</sub>) intensity. The color wedge scales the velocity range from 40 to  $80 \text{ km s}^{-1}$ . The contours outline the intensity level of  $4 \text{ Jy beam}^{-1} \text{ km s}^{-1}$  for both images.

Fig. 3 shows the velocity field of H<sub>2</sub>CO emission. The kinematical structure observed from the lower transition (see Fig. 3(a)) in Sgr B2(M) is relatively simple, consisting of a red spot 5" SE of the compact core and the NW arch structure. The red spot (red-shifted emission, see

also the spectrum M4 in Fig. 2) appears to be a fast moving compact component ( $V_{lsr} \sim 100$  km s $^{-1}$ ) ejected from the core. The appearance of the NW arch (blue-shifted emission) suggests that the gas is undergoing a complicated infalling process through interacting with the outflow while spiraling into the core rather than simply free falling. There is a velocity gradient in NS in Sgr B2(N) (see also Fig. 3(a)). Based on the HC<sub>3</sub>N observations, Lis et al. (1993) [8] argued that the NS velocity gradient in Sgr B2(N) traces the rotation. The kinematics of the lower H<sub>2</sub>CO transition in emission gas of Sgr B2(N) is likely dominated by the gas rotating around the core. The velocity field of the higher transition gas appears to trace the outflow better (see Fig. 3(b)). The red-shifted outflow SE to the core of Sgr B2(M) is clearly present. The kinematics of the NW arch of Sgr B2(M) observed in the high transition gas appears to be similar to that observed in the lower transition gas. The outflow in Sgr B2(N) was observed in SW direction [8]. The SE-NW velocity gradient of the high transition gas in Sgr B2(N) could be caused by the combination of the rotation and outflow.

Based on the line ratio of  $F_{303-202}/F_{321-220}$  from the spectra, most of the gas in the Sgr B2 region does not satisfy the LTE condition. Assuming the molecular cloud is in plane-parallel geometry, the molecular excitation in non-LTE has been modelled based on an LVG approximation (e.g. [14],[16]). The non-LTE calculation suggests that the absorbing gas of the compact cores have a kinetic temperature of  $\sim 40$  K and H<sub>2</sub> density of  $\sim 10^7$  cm $^{-3}$ . A higher kinetic temperature ( $\geq 50$  K) and relatively lower H<sub>2</sub> density ( $\sim 10^6$  cm $^{-3}$ ) are needed to explain the emission gas both residing in the cores (probably tracing the outflows) and surrounding the cores. The detected larger-scale emission appears to be from a warm envelope, and absorbing gas appears to trace cold dense condensations associated with the massive star forming cores.

### 3. Conclusions

H<sub>2</sub>CO lines and continuum at 1.3 mm were observed with SMA. The infalling gas was detected through the red-shifted absorbing gas against the continuum in Sgr B2 compact cores and their associated dusty clumps and filament Z10.24. The gas clumps in emission were also observed in both H<sub>2</sub>CO lines. Based on an LVG model, our analysis suggests that the gas in Sgr B2 complex consists of cold dense cores and a warm but less dense envelope. The red-shifted outflow in Sgr B2(M) is observed in H<sub>2</sub>CO (3<sub>21</sub>-2<sub>20</sub>) line and appears to be excited by C-shock.

### Acknowledgments

We thank all the SMA staff of SAO and ASIAA for making SMA observations possible.

### References

- [1] Gaume R A & Glaussen M J 1990 *ApJ* **351** 538
- [2] Gaume R A, Glaussen M J, De Pree C G *et al.* 1995 *ApJ* **449** 663
- [3] Mehringer D M, Palmer P, Goss W M 1993 *ApJ* **412** 68
- [4] De Pree C G, Gaume R A, Goss W M *et al.* 1995 *ApJ* **451** 284
- [5] De Pree C G, Gaume R A, Goss W M *et al.* 1996 *ApJ* **464** 788
- [6] De Pree C G, Goss W M, Gaume R A *et al.* 1998 *ApJ* **500** 84
- [7] Vogel S N, Genzel R, Palmer P, 1987, *ApJ*, **316** 243
- [8] Lis D C, Goldsmith P F, Carlstrom, J E *et al.* 1993 *ApJ* **402** 238
- [9] Kuan Y J & Snyder L E 1994 *ApJS* **94** 651
- [10] Kuan Y J & Snyder L E 1996 *ApJ* **470** 981
- [11] Kuan Y J, Mehringer D M, Snyder L E 1996 *ApJ* **459** 619
- [12] Liu S Y & Snyder L E 1998 *ApJ* **523** 683
- [13] Mangum J G & Wootten A 1993 *ApJ* **89** 123
- [14] Evans N J, Davis J H, Plambeck R L 1979 *ApJ* **227** L25
- [15] McKee C F, Chernoff D F and Hollenbach D J 1984, in Proc. 16th ESLAB Symp. Galactic and Extragalactic infrared Spectroscopy, ed. M. Kessler & J. Phillips (Dordrechi:Reidel), 103
- [16] Scoville N Z & Solomon P M 1974 *ApJ* **187** L71